

Article

Kurchatovite and Clinokurchatovite, Ideally CaMgB_2O_5 : An Example of Modular Polymorphism

Yulia A. Pankova ¹, Sergey V. Krivovichev ^{1,2,*} , Igor V. Pekov ³, Edward S. Grew ⁴
and Vasilij O. Yapaskurt ³

¹ Department of Crystallography, Institute of Earth Sciences, St. Petersburg State University, University Emb. 7/9, 199034 St. Petersburg, Russia; yulika1314@gmail.com

² Nanomaterials Research Centre, Kola Science Centre, Russian Academy of Sciences, Fersmana 14, 184209 Apatity, Russia

³ Faculty of Geology, Moscow State University, Vorob'evy Gory, 119991 Moscow, Russia; igorpekov@mail.ru (I.V.P.); yvo72@geol.msu.ru (V.O.Y.)

⁴ School of Earth and Climate Sciences, University of Maine, 5790 Bryand Global Science Center, Orono, ME 04469, USA; esgrew@maine.edu

* Correspondence: s.krivovichev@spbu.ru or krivovichev@admksk.apatity.ru; Tel.: +7-81555-7-53-50

Received: 4 July 2018; Accepted: 26 July 2018; Published: 2 August 2018



Abstract: Kurchatovite and clinokurchatovite, both of ideal composition CaMgB_2O_5 , from the type localities (Solongo, Buryatia, Russia, and Sayak-IV, Kazakhstan, respectively) have been studied using electron microprobe and single-crystal X-ray diffraction methods. The empirical formulae of the samples are $\text{Ca}_{1.01}\text{Mg}_{0.87}\text{Mn}_{0.11}\text{Fe}^{2+}_{0.02}\text{B}_{1.99}\text{O}_5$ and $\text{Ca}_{0.94}\text{Mg}_{0.91}\text{Fe}^{2+}_{0.10}\text{Mn}_{0.04}\text{B}_{2.01}\text{O}_5$ for kurchatovite and clinokurchatovite, respectively. The crystal structures of the two minerals are similar and based upon two-dimensional blocks arranged parallel to the *c* axis in kurchatovite and parallel to the *a* axis in clinokurchatovite. The blocks are built up from diborate B_2O_5 groups, and Ca^{2+} and Mg^{2+} cations in seven- and six-fold coordination, respectively. Detailed analysis of geometrical parameters of the adjacent blocks reveals that symmetrically different diborate groups have different degrees of conformation in terms of the δ angles between the planes of two BO_3 triangles sharing a common O atom, featuring two discrete sets of the δ values of ca. 55° (B' blocks) and 34° (B'' blocks). The stacking of the blocks in clinokurchatovite can be presented as ... $(+\text{B}')(+\text{B}'')(+\text{B}')(+\text{B}'')$... or $[(+\text{B}')(+\text{B}'')]$, whereas in kurchatovite it is more complex and corresponds to the sequence ... $(+\text{B}')(+\text{B}'')(+\text{B}')(-\text{B}')(-\text{B}'')(-\text{B}')(+\text{B}')(+\text{B}'')(+\text{B}')(-\text{B}')(-\text{B}'')(-\text{B}')$... or $[(+\text{B}')(+\text{B}'')(+\text{B}')(-\text{B}')(-\text{B}'')(-\text{B}')]$. The $\text{B}'\text{:B}''$ ratios for clinokurchatovite and kurchatovite are 1:1 and 2:1, respectively. According to this description, the two minerals cannot be considered as polytypes and their mutual relationship corresponds to the term modular polymorphs. From the viewpoint of information-based measures of structural complexity, clinokurchatovite ($I_G = 4.170$ bits/atom and $I_{G,\text{total}} = 300.235$ bits/cell) is structurally simpler than kurchatovite ($I_G = 4.755$ bits/atom and $I_{G,\text{total}} = 1027.056$ bits/cell). The high structural complexity of kurchatovite can be inferred from the modular character of its structure. The analysis of structural combinatorics in terms of the modular approach allows to construct the whole family of theoretically possible “kurchatovite”-type structures that bear the same structural features common for kurchatovite and clinokurchatovite. However, the crystal structures of the latter minerals are the simplest and are the only ones that have been observed in nature. The absence of other possible structures is remarkable and can be explained by either the maximum-entropy of the least-action fundamental principles.

Keywords: kurchatovite; clinokurchatovite; crystal structure; borate; polymorphism; polytypism; structural complexity; structural combinatorics; configurational entropy; least-action principle

1. Introduction

Kurchatovite and clinokurchatovite are rare anhydrous Ca-Mg borates reported in skarns from several localities in Russia, Kazakhstan, Afghanistan and Japan [1–4].

Kurchatovite was discovered in a vesuvianite-garnet calc-silicate skarn in the Solongo boron and iron deposit, Buryatia (Siberia, Russia), in close association with sphalerite, magnetite and turneaureite-johnbaumite series arsenates [1,5,6]. It was interpreted to have formed as an early mineral when boron was introduced with postmagmatic fluids. A wet chemical analysis after deduction of impurities gave the following formula calculated based on five oxygen atoms per formula unit (*pfu*): $\text{Ca}_{0.955}(\text{Mg}_{0.816}\text{Mn}_{0.183}\text{Fe}_{0.040})_{\Sigma 1.039}\text{B}_{2.005}\text{O}_5$. Single-crystal X-ray diffraction study gave orthorhombic symmetry with $a = 11.15(0.02)$, $b = 36.4(0.1)$, and $c = 5.55(0.01)$ Å in the original description; whereas Yakubovich et al. [7] gave the space group as $Pc2_1b$ when the structure was refined. The possibility of a monoclinic analogue was first suggested by syntheses [8] and presence of twins [9–11], and subsequently confirmed by single-crystal studies and crystal-structure refinements of synthetic and natural material, including a synthetic Ca-Mn analogue [7,12–15], eventually leading to the formal description of clinokurchatovite as a new mineral [16]. The type locality is the Sayak-IV gold and copper deposit, Balkhash Region, Kazakhstan, where clinokurchatovite occurs in skarn with calcite, harkerite, grossular-andradite garnet, magnetite and, locally, ludwigite. Other reliably reported localities of clinokurchatovite are the Novofrolovskoe copper deposit, Northern Urals, and the Titovskoe boron deposit, Polar Yakutia, Siberia, both in Russia [1].

Kurchatovite from the Fuka mine, Okayama Prefecture, Japan, ranges in chemical composition (with negligible Mn) from the almost end member (2 mol % CaFeB_2O_5) to the Fe-dominant analogue (53 mol % CaFeB_2O_5); there is first report of a kurchatovite-type mineral with $\text{Fe} > \text{Mg}$ [4].

The crystal structures of kurchatovite and clinokurchatovite have been re-investigated by Callegari et al. [17], who reported for kurchatovite the space group $Pbca$. According to Yakubovich et al. [7] and Belokoneva et al. [18], the crystal structures of kurchatovite and clinokurchatovite could be considered as polytypes. Callegari et al. [17] mentioned this hypothesis as a possibility, leaving it aside “to the experts in this manner”. However, if kurchatovite and clinokurchatovite are polytypes, then they should be considered as one mineral species existing in two polytypic varieties, which would warrant the discreditation of one of them and re-definition of the other.

The aim of the present paper is to report on the results of crystal-structure studies of kurchatovite and clinokurchatovite, to analyze their structural relations from the viewpoint of the concepts of polymorphism and polytypism, and to examine the validity of the two minerals as separate mineral species in the frame of actual approach accepted in mineral nomenclature.

2. Materials and Methods

2.1. Description of Samples

The samples examined in the present work originate from the collection of one of the authors (I.V.P.), #425 (kurchatovite) and #428 (clinokurchatovite). Both samples are from the type localities of these minerals and were received from the senior author of their first descriptions, Prof. Svetlana Vyacheslavovna Malinko (1927–2002). The clinokurchatovite sample is a part of the holotype specimen studied by Malinko and Pertsev [16].

Sample #425 is a fragment of drillcore of a borehole from the Solongo deposit. Kurchatovite occurs as colorless to greyish equant grains up to 3 mm across. It is a major constituent of a massive borate-rich rock that also contains sakhaite, calcite and magnetite and is crosscut by vimsite veinlets.

Sample #428 is a fragment of drill core from a borehole in the Sayak-IV deposit. Clinokurchatovite forms colorless tabular grains up to 2 mm across associated with harkerite and minor magnetite in a massive skarn rock consisting mainly of calcite and andradite.

2.2. Chemical Composition

The chemical compositions of kurchatovite and clinokurchatovite were studied using a JEOL JSM-6480LV (JEOL, Japan) scanning electron microscope equipped with an INCA-Wave 500 wavelength-dispersive spectrometer (Laboratory of Analytical Techniques of High Spatial Resolution, Department of Petrology, Moscow State University). The WDS mode was used, with an acceleration voltage of 20 kV and a beam current of 10 nA; electron beam was rastered to $5 \mu\text{m} \times 5 \mu\text{m}$ area. The standards used were as follows: wollastonite (Ca), MgO (Mg), Mn (Mn), Fe (Fe), and BN (B). Contents of other elements with atomic numbers higher than carbon were below detection limits.

Table 1 provides the summary of analytical results (the averages of eight- and six-point analyses for kurchatovite and clinokurchatovite, respectively). The resulting empirical formulae obtained in our study can be written as $\text{Ca}_{1.01}\text{Mg}_{0.87}\text{Mn}_{0.11}\text{Fe}^{2+}_{0.02}\text{B}_{1.99}\text{O}_5$ for kurchatovite and $\text{Ca}_{0.94}\text{Mg}_{0.91}\text{Fe}^{2+}_{0.10}\text{Mn}_{0.04}\text{B}_{2.01}\text{O}_5$ for clinokurchatovite, and both are in good agreement with the previous studies and the results of crystal-structure analysis.

Table 1. Chemical composition of kurchatovite from Solongo (#425) and clinokurchatovite from Sayak-IV (#428).

| Constituent | #425 | e.s.d. * | #428 | e.s.d. |
|--|-------|----------|-------|--------|
| wt % | | | | |
| CaO | 32.74 | 1.12 | 30.82 | 0.98 |
| MgO | 20.12 | 0.76 | 21.58 | 0.81 |
| MnO | 4.54 | 0.12 | 1.73 | 0.09 |
| FeO | 0.84 | 0.06 | 4.05 | 0.54 |
| B ₂ O ₃ | 40.04 | 2.44 | 40.89 | 2.01 |
| Total | 98.28 | | 99.07 | |
| calculated based on 5 O atoms per formula unit | | | | |
| Ca | 1.01 | | 0.94 | |
| Mg | 0.87 | | 0.91 | |
| Mn | 0.11 | | 0.04 | |
| Fe | 0.02 | | 0.10 | |
| B | 1.99 | | 2.01 | |

* e.s.d. = estimated standard deviation.

2.3. Single-Crystal X-ray Diffraction

The crystals of kurchatovite and clinokurchatovite selected for data collection were mounted on a Bruker «SMART APEX» X-ray diffractometer operated at 50 kV and 40 mA and equipped with the I μ S microfocuss source. More than a hemisphere of three-dimensional data was collected for each crystal using monochromatic MoK α X-radiation, with frame widths of 0.5°, and with a 10 s count for each frame. The unit-cell parameters (Table 2) were refined using least-squares techniques. The intensity data were integrated and corrected for Lorentz, polarization, and background effects using the Bruker programs APEX and XPREP. An analytical multiscan absorption correction was performed using SADABS. The observed systematic absences were consistent with the space groups *Pbca* and *P2₁/c* for kurchatovite and clinokurchatovite, respectively, in agreement with the previous report by Callegari et al. [17]. The refinements converged to $R_1 = 0.0265$ and 0.0287 based on 4240 and 2480 unique reflections for kurchatovite and clinokurchatovite, respectively. The SHELX program package was used for all structural calculations [19]. The final atomic coordinates and isotropic displacement parameters are given in Tables 3 and 4 and selected interatomic distances are in Tables 5 and 6.

Table 2. Crystal data and structure refinement for kurchatovite and clinokurchatovite.

| | | Kurchatovite | Clinokurchatovite |
|---|---------------------------|--|----------------------------|
| Crystallographic Data | | | |
| Crystal system | | orthorhombic | Monoclinic |
| Space group | | <i>Pbca</i> | <i>P2₁/c</i> |
| Unit-cell parameters | <i>a</i> , Å | 11.1543(5) | 12.330(1) |
| | <i>b</i> , Å | 5.5078(2) | 11.147(1) |
| | <i>c</i> , Å | 36.357(2) | 5.5154(5) |
| | β , deg. | 90 | 101.604(2) |
| | <i>V</i> , Å ³ | 2233.6(2) | 742.56(12) |
| Z | | 12 | 4 |
| Density (g/cm ³) | | 3.051 | 3.063 |
| Absorption coefficient (mm ⁻¹) | | 2.249 | 2.348 |
| Crystal size (mm ³) | | 0.25 × 0.15 × 0.07 | 0.14 × 0.08 × 0.06 |
| Data Collection Parameters | | | |
| Temperature, K | | 296(2) | 296(2) |
| Radiation type, wavelength | | MoK α , 0.71073 | |
| 2 θ angles range, deg. | | 1.120–36.270 | 1.686–36.194 |
| <i>h</i> , <i>k</i> , <i>l</i> values range | | −18 → 18, −8 → 9, −54 → 60 | −20 → 20, −18 → 18, −9 → 7 |
| Reflections collected | | 37,908 | 13,239 |
| Unique reflections (<i>R</i> _{int}) | | 5260 (0.0311) | 3425 (0.0291) |
| Observed reflections (>4 σ <i>F</i> _{<i>o</i>}) | | 4240 | 2480 |
| Structure-Refinement Parameters | | | |
| Refinement method | | Full-matrix least-square analysis of <i>F</i> ² | |
| Weight coefficients <i>a</i> , <i>b</i> | | 0.0328, 1.3584 | 0.0290, 0.2749 |
| <i>R</i> ₁ [<i>F</i> > 4 σ (<i>F</i>)], <i>wR</i> ₂ [<i>F</i> > 4 σ (<i>F</i>)] | | 0.0265, 0.0656 | 0.0287, 0.0633 |
| <i>R</i> ₁ [all data], <i>wR</i> ₂ [all data] | | 0.0392, 0.0706 | 0.0505, 0.0716 |
| No. of refined parameters | | 251 | 165 |
| <i>S</i> | | 1.032 | 1.014 |
| ρ_{\max} , ρ_{\min} , <i>e</i> ·Å ⁻³ | | 0.58, −0.43 | 0.49, −0.51 |

Table 3. Atomic coordinates, site occupancies and isotropic displacement parameters (Å²) for kurchatovite.

| Atom | Occupancy | <i>x</i> | <i>y</i> | <i>z</i> | <i>U</i> _{eq} |
|------|---------------------------------------|------------|------------|-------------|------------------------|
| Ca1 | Ca | 0.61922(2) | 0.87281(5) | 0.197511(7) | 0.00938(5) |
| Ca2 | Ca | 0.62704(2) | 0.11587(4) | 0.029585(7) | 0.00855(5) |
| Ca3 | Ca | 0.38191(2) | 0.68481(5) | 0.135926(7) | 0.00851(5) |
| Mg1 | Mg _{0.83} Mn _{0.17} | 0.36899(3) | 0.90620(7) | 0.24556(1) | 0.0071(1) |
| Mg2 | Mg _{0.85} Mn _{0.15} | 0.37184(3) | 0.13959(6) | 0.07913(1) | 0.0070(1) |
| Mg3 | Mg _{0.84} Mn _{0.16} | 0.62831(3) | 0.63546(6) | 0.08798(1) | 0.0069(1) |
| B1 | B | 0.6165(1) | 0.9056(2) | 0.27635(4) | 0.0075(2) |
| B2 | B | 0.3801(1) | 0.3481(2) | 0.00382(4) | 0.0075(2) |
| B3 | B | 0.3758(1) | 0.6224(2) | 0.05821(4) | 0.0076(2) |
| B4 | B | 0.6232(1) | 0.4041(2) | 0.16340(4) | 0.0074(2) |
| B5 | B | 0.3769(1) | 0.1430(2) | 0.16971(4) | 0.0077(2) |
| B6 | B | 0.6158(1) | 0.1422(2) | 0.10852(4) | 0.0076(2) |
| O1 | O | 0.60741(8) | 0.1717(2) | 0.14686(2) | 0.0099(2) |
| O2 | O | 0.39113(8) | 0.3799(2) | 0.18516(2) | 0.0096(2) |
| O3 | O | 0.33020(8) | 0.1304(2) | 0.13512(2) | 0.0097(2) |
| O4 | O | 0.69551(7) | 0.7625(2) | 0.25775(2) | 0.0086(2) |
| O5 | O | 0.41787(8) | 0.1526(2) | 0.02313(2) | 0.0086(2) |
| O6 | O | 0.62748(8) | 0.4165(2) | −0.01965(3) | 0.0096(2) |
| O7 | O | 0.69533(7) | 0.2813(2) | 0.08927(2) | 0.0086(2) |
| O8 | O | 0.54422(8) | 0.9772(2) | 0.09097(2) | 0.0090(2) |
| O9 | O | 0.45005(7) | 0.4882(2) | 0.08012(2) | 0.0086(2) |
| O10 | O | 0.66730(8) | 0.4040(2) | 0.19815(2) | 0.0109(2) |
| O11 | O | 0.65926(8) | 0.6685(2) | 0.03147(2) | 0.0100(2) |
| O12 | O | 0.45486(8) | 0.5679(2) | 0.24184(2) | 0.0096(2) |
| O13 | O | 0.40938(8) | 0.9429(2) | 0.18909(2) | 0.0084(2) |
| O14 | O | 0.30194(7) | 0.7933(2) | 0.07285(2) | 0.0083(2) |
| O15 | O | 0.59502(8) | 0.6100(2) | 0.14478(2) | 0.0090(2) |

Table 4. Atomic coordinates, site occupancies and isotropic displacement parameters (\AA^2) for clinokurchatovite.

| Atom | Occupancy | x | y | z | U_{eq} |
|------|---------------------------------------|------------|-------------|------------|------------|
| Ca1 | Ca | 0.08981(2) | 0.87295(2) | 0.15613(5) | 0.00945(6) |
| Ca2 | Ca | 0.40709(2) | 0.11838(3) | 0.86795(5) | 0.00964(6) |
| Mg1 | Mg _{0.82} Fe _{0.18} | 0.23725(3) | 0.12783(3) | 0.24798(7) | 0.0074(1) |
| Mg2 | Mg _{0.85} Fe _{0.15} | 0.26425(3) | 0.87208(4) | 0.75442(7) | 0.0075(1) |
| B1 | B | 0.1737(1) | 0.1244(1) | 0.7008(3) | 0.0085(3) |
| B2 | B | 0.3274(1) | 0.8833(1) | 0.2898(3) | 0.0080(2) |
| B3 | B | 0.0110(1) | 0.1199(1) | 0.3523(3) | 0.0081(3) |
| B4 | B | 0.4910(1) | 0.8758(1) | 0.6265(3) | 0.0081(2) |
| O1 | O | 0.21777(8) | 0.19770(9) | 0.8923(2) | 0.0092(2) |
| O2 | O | 0.26893(8) | 0.80443(9) | 0.4030(2) | 0.0090(2) |
| O3 | O | 0.23931(8) | 0.04971(9) | 0.5970(2) | 0.0094(2) |
| O4 | O | 0.27471(8) | −0.04466(9) | 0.1016(2) | 0.0095(2) |
| O5 | O | 0.05777(8) | 0.12793(9) | 0.6085(2) | 0.0103(2) |
| O6 | O | 0.44314(8) | 0.89021(10) | 0.3708(2) | 0.0107(2) |
| O7 | O | 0.06922(8) | 0.08205(9) | 0.1841(2) | 0.0090(2) |
| O8 | O | 0.43363(8) | −0.09361(9) | 0.8032(2) | 0.0091(2) |
| O9 | O | 0.09551(8) | 0.84098(9) | 0.7140(2) | 0.0105(2) |
| O10 | O | 0.40463(8) | 0.16960(9) | 0.3182(2) | 0.0107(2) |

Table 5. Selected bond lengths (\AA) for the crystal structure of kurchatovite.

| | | | | | |
|---------|-----------|---------|----------|---------|----------|
| Ca1-O10 | 2.388(1) | Ca2-O5 | 2.354(1) | Ca3-O3 | 2.385(1) |
| Ca1-O13 | 2.392(2) | Ca2-O11 | 2.402(1) | Ca3-O13 | 2.419(1) |
| Ca1-O15 | 2.418(1) | Ca2-O6 | 2.438(1) | Ca3-O9 | 2.422(1) |
| Ca1-O4 | 2.427(1) | Ca2-O5 | 2.472(1) | Ca3-O15 | 2.434(1) |
| Ca1-O1 | 2.474(1) | Ca2-O7 | 2.474(1) | Ca3-O2 | 2.460(1) |
| Ca1-O12 | 2.588(1) | Ca2-O11 | 2.491(1) | Ca3-O3 | 2.521(1) |
| Ca1-O10 | 2.637(1) | Ca2-O8 | 2.533(1) | Ca3-O14 | 2.532(1) |
| <Ca1-O> | 2.475 | <Ca2-O> | 2.452 | <Ca3-O> | 2.453 |
| Mg1-O10 | 2.0862(1) | Mg2-O14 | 2.073(1) | Mg3-O7 | 2.089(1) |
| Mg1-O4 | 2.0936(1) | Mg2-O3 | 2.088(1) | Mg3-O11 | 2.091(1) |
| Mg1-O4 | 2.0941(1) | Mg2-O5 | 2.101(1) | Mg3-O15 | 2.103(1) |
| Mg1-O12 | 2.0994(1) | Mg2-O9 | 2.109(1) | Mg3-O8 | 2.106(1) |
| Mg1-O13 | 2.1116(1) | Mg2-O14 | 2.127(1) | Mg3-O7 | 2.126(1) |
| Mg1-O12 | 2.2054(1) | Mg2-O8 | 2.164(1) | Mg3-O9 | 2.166(1) |
| <Mg1-O> | 2.115 | <Mg2-O> | 2.110 | <Mg3-O> | 2.114 |
| B1-O4 | 1.362(2) | B2-O5 | 1.353(2) | B3-O14 | 1.359(2) |
| B1-O12 | 1.367(2) | B2-O11 | 1.359(2) | B3-O9 | 1.366(2) |
| B1-O2 | 1.410(2) | B2-O6 | 1.421(2) | B3-O6 | 1.419(2) |
| <B1-O> | 1.380 | <B2-O> | 1.378 | <B3-O> | 1.381 |
| B4-O10 | 1.356(2) | B5-O13 | 1.357(2) | B6-O7 | 1.365(2) |
| B4-O15 | 1.358(2) | B5-O3 | 1.363(2) | B6-O8 | 1.368(2) |
| B4-O1 | 1.425(2) | B5-O2 | 1.425(2) | B6-O1 | 1.407(2) |
| <B4-O> | 1.380 | <B5-O> | 1.382 | <B6-O> | 1.380 |

Table 6. Selected bond lengths (\AA) for the crystal structure of kurchatovite.

| | | | | | |
|---------|-----------|---------|-----------|--------|------------|
| Ca1-O7 | 2.3531(1) | Mg1-O10 | 2.0746(1) | B1-O1 | 1.3594(2) |
| Ca1-O9 | 2.4052(1) | Mg1-O1 | 2.0789(1) | B1-O3 | 1.3645(2) |
| Ca1-O5 | 2.4384(1) | Mg1-O7 | 2.0936(1) | B1-O5 | 1.4180(2) |
| Ca1-O2 | 2.4709(1) | Mg1-O3 | 2.1083(1) | <B1-O> | 1.381 |
| Ca1-O7 | 2.4774(1) | Mg1-O1 | 2.1334(1) | B2-O2 | 1.3649(2) |
| Ca1-O9 | 2.4791(1) | Mg1-O4 | 2.1708(1) | B2-O4 | 1.3685(2) |
| Ca1-O4 | 2.5311(1) | <Mg1-O> | 2.110 | B2-O6 | 1.4097(2) |
| <Ca1-O> | 2.451 | | | <B2-O> | 1.381 |
| | | Mg2-O9 | 2.0764(1) | B3-O7 | 1.3499(2) |
| Ca2-O10 | 2.3789(1) | Mg2-O8 | 2.0867(1) | B3-O9 | 1.3623(2) |
| Ca2-O8 | 2.4060(1) | Mg2-O2 | 2.0911(1) | B3-O5 | 1.4175(2) |
| Ca2-O3 | 2.4198(1) | Mg2-O4 | 2.1084(1) | <B3-O> | 1.377 |
| Ca2-O8 | 2.4220(1) | Mg2-O2 | 2.1279(1) | B4-O8 | 1.3577(2) |
| Ca2-O6 | 2.4759(1) | Mg2-O3 | 2.1591(1) | B4-O10 | 1.3598(2) |
| Ca2-O1 | 2.5249(1) | <Mg2-O> | 2.108 | B4-O6 | 1.4240(2)- |
| Ca2-O10 | 2.5541(1) | | | <B4-O> | 1.359 |
| <Ca2-O> | 2.455 | | | | |

3. Results

The crystal structures of kurchatovite and clinokurchatovite are shown in Figures 1a and 2a, respectively. Their basic structural features are the same as reported by Yakubovich et al. [7,12,13], Simonov et al. [15], and Callegari et al. [17]. Mg^{2+} cations are coordinated octahedrally with the average $\langle Mg-O \rangle$ bond lengths in the range of 2.108–2.115 Å (individual bond lengths vary from 2.073 to 2.205 Å). Ca^{2+} cations are coordinated by seven O atoms each with the $\langle Ca-O \rangle$ bond lengths in the range of 2.451–2.475 Å. B^{3+} cations are coordinated by three O atoms each to form BO_3 triangles ($\langle B-O \rangle = 1.359$ – 1.382 Å). Two BO_3 triangles share common O_{br} atoms (O_{br} = bridging O atom) to form $[B_2O_5]^{4-}$ diborate group. The $B-O_{br}$ bonds are essentially longer (1.407–1.425 Å) than the $B-O_t$ bonds (1.353–1.369 Å; O_t = terminal O atoms), in agreement with the observations by Filatov and Bubnova [20]. The $B-O_{br}-B$ angles in the B_2O_5 groups are in the range 118.6–122.4°.

According to the description first developed by Yakubovich et al. [7], the crystal structures of the two minerals are similar and based upon two-dimensional blocks of the kind shown in Figure 3a. The blocks are about 6 Å thick and are arranged perpendicular to the c axis in kurchatovite and parallel to (100) in clinokurchatovite. Callegari et al. [17] proposed different approach to the structure description by splitting the crystal structures into thinner blocks (“monoclinic modules”) consisting of B_2O_5 groups, BO_3 triangles, and Ca^{2+} and Mg^{2+} cations. In her detailed OD-analysis of kurchatovite and clinokurchatovite, Belokoneva [18] subdivided in the two structures two layers, $MgBO_{2.5}$ (L_1) and $CaBO_{2.5}$ (L_2), with local symmetries $P(b)c2_1$ and $P(1)2_1/c1$, respectively. The L_1 layer contains $B1O_3$ triangles and Mg^{2+} ions, whereas the L_2 layer contains $B2O_3$ triangles and Ca^{2+} ions. The layers alternate to form L_1L_2 pairs, which stack in the $+1/4, +1/4, +1/4 \dots$ sequence in clinokurchatovite [a maximum degree of order 1 (MDO1) polytype] and in the $+1/4, +1/4, +1/4, -1/4, -1/4, -1/4 \dots$ sequence in kurchatovite, where $+1/4$ and $-1/4$ symbolize shifts and orientations of the layers along the b axis in kurchatovite and the c axis in clinokurchatovite.

Despite their relevance and simplicity, the approaches developed by Callegari et al. [17] and Belokoneva [18] possess several disadvantages: (1) both approaches imply “splitting” of B_2O_5 groups into single BO_3 triangles, which is theoretically feasible, but physically unrealistic; (2) Belokoneva’s approach takes into account only the B1 and B2 sites, whereas, in clinokurchatovite, there are four B sites; (3) both approaches are unable to explain the absence of the “hypothetical protostructure” derived by Yakubovich et al. [7], i.e., the monoclinic structure consisting of one block only, i.e., with $a \sim 6.2$ Å if one uses the monoclinic setting of clinokurchatovite.

To develop a transparent and reliable method for the analysis of relationships between kurchatovite and clinokurchatovite, the two structures can first be analyzed in terms of the arrangements of the B_2O_5 groups (Figures 1b and 2b).

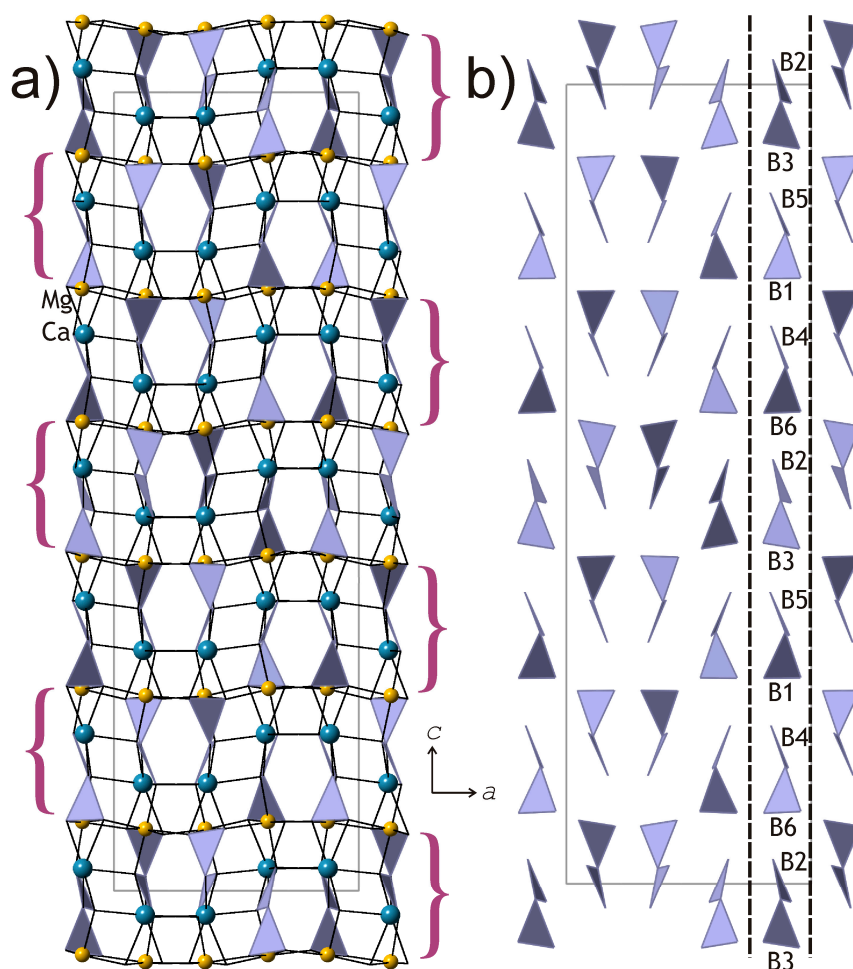


Figure 1. The crystal structure of kurchatovite projected along the b axis (a) and the arrangement of B_2O_5 groups (b). The curved brackets in (a) denote the basic two-dimensional blocks, whereas the dashed lines in (b) indicate directions of division of the structure into single slices consisting of diborate groups.

In turn, the two arrangements can be split into two-dimensional slices indicated by dashed lines in Figures 1b and 2b. The arrangement of the B_2O_5 groups in the plane of the slices (Figure 4a,c) clearly demonstrates the relations between the two structures in terms of the sequence of the groups along the direction of the layer stacking. The Ca^{2+} and Mg^{2+} cations lie in the plane of the slices, possessing five- and four-fold coordination, respectively (Figure 4b,d). The dot-and-dash lines in Figure 4a,c show the separation of the slices into 6 Å-blocks corresponding to “protostructure” by Yakubovich et al. [7]. The description of the two structures in terms of these blocks is physically realistic, since it does not imply hypothetical splitting of diborate groups into single BO_3 triangles.

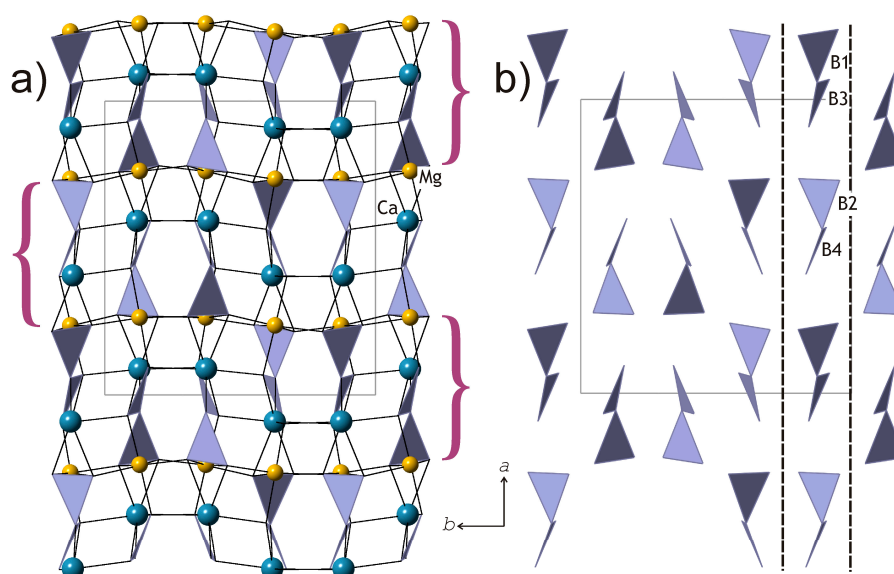


Figure 2. The crystal structure of clinokurchatovite projected along the c axis (a) and the arrangement of B_2O_5 groups (b). The dashed lines in (b) indicate directions of division of the structure into single slices consisting of diborate groups.

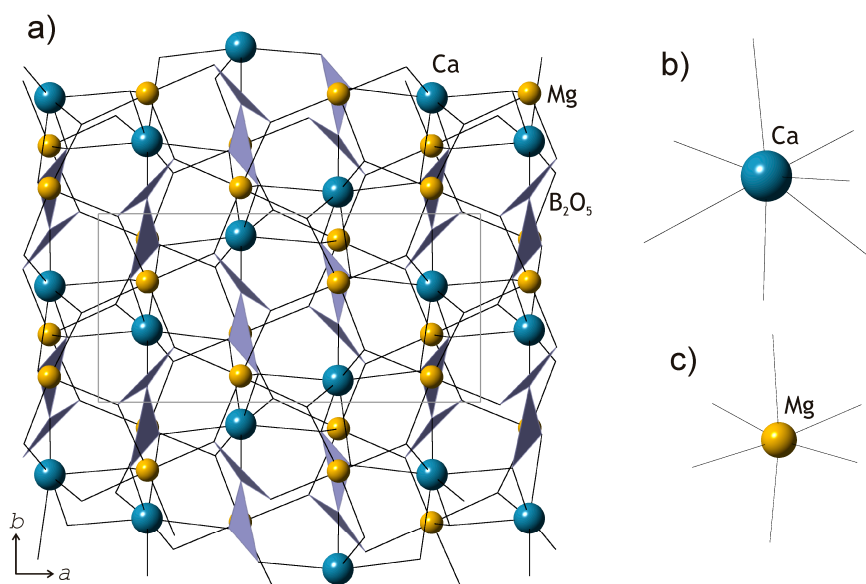


Figure 3. The structure topology of the 6 Å-block in the crystal structures of kurchatovite and clinokurchatovite (a; the picture corresponds to one of the symmetrically independent blocks in kurchatovite) and the coordination figures of Ca (b) and Mg (c) atoms.

The proposed approach appears to support a polytypic relationship between kurchatovite and clinokurchatovite, since both are based upon the layers of the same kind stacked in different sequences. However, detailed analysis of geometrical parameters of the adjacent 6 Å-blocks reveals a more complicated situation. As mentioned above, the geometries of the B_2O_5 groups in the two structures are almost identical with the B–O bond lengths and valence angles varying over very narrow ranges. However, a closer investigation of symmetrically different diborate groups demonstrates that they have different degrees of conformation in terms of the δ angles between the planes of two BO_3 triangles sharing a common O atom. The diagrams in Figure 5 show that the B_2O_5 groups belong to two discrete types with the δ values of ca. 55° and 34° , respectively.

In both minerals, each 6 Å-block consists exclusively of diborate groups with the same δ value of either $55.5 \pm 0.5^\circ$ or $33.7 \pm 0.5^\circ$. To make the distinction clear, we denote the 55° block as B' , and the 34° block as B'' . Thus, taking into account the directions of the blocks along the c axis in clinokurchatovite and the b axis in kurchatovite symbolized as + or – (related by the 180° rotation around the vertical axis), the stacking of the 6 Å-blocks in clinokurchatovite can be described as ... $(+B')(+B'')(+B')(+B'')$... or $[(+B')(+B'')]$. In contrast, the stacking in kurchatovite is more complex and corresponds to the sequence ... $(+B')(+B'')(+B')(-B')(-B'')(-B')(+B')(+B'')(+B')(-B')(-B'')(-B')$... or $[(+B')(+B'')(+B')(-B')(-B'')(-B')]$. The $B':B''$ ratios for clinokurchatovite and kurchatovite are 1:1 and 2:1, respectively. It is worthy to note that the proposed description of the two structures in terms of two different layers allows for the explanation of the absence of the “protostructure” by Yakubovich et al. [7]. In fact, clinokurchatovite is the simplest structure possible in this mineral group (see also below).

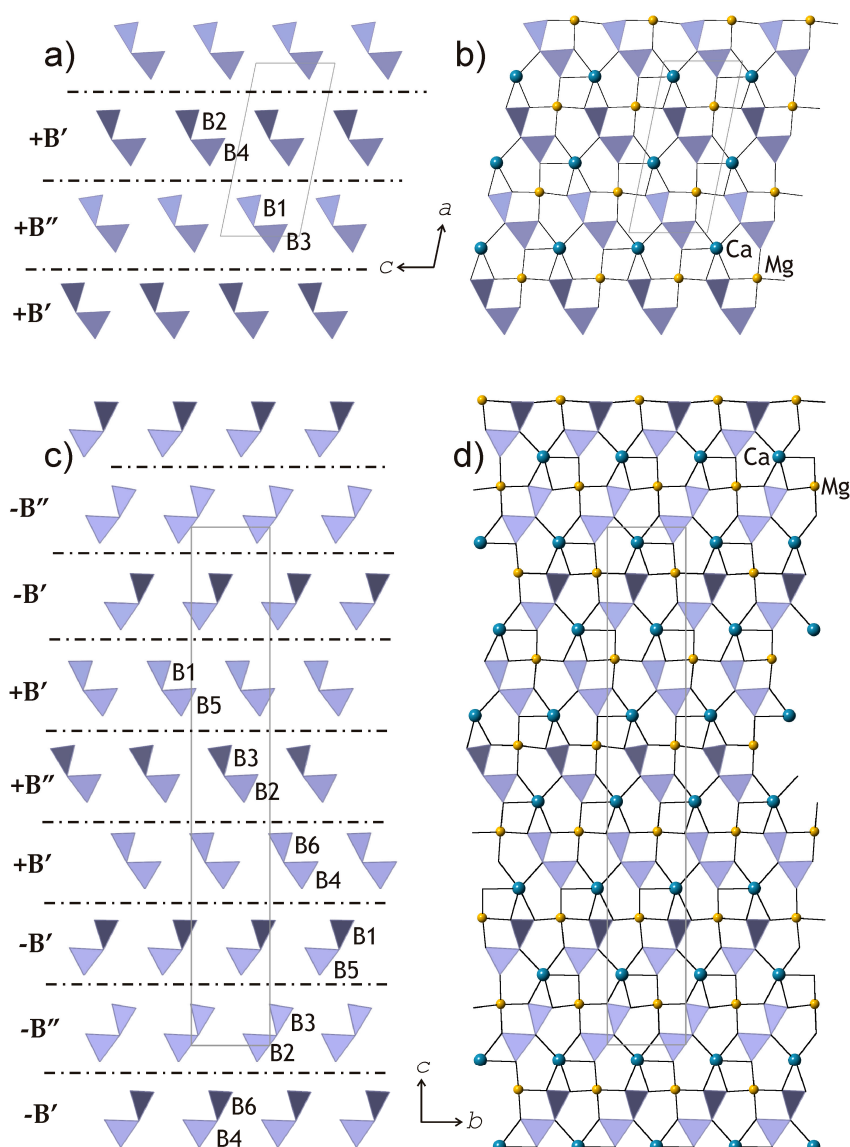


Figure 4. The slices of the crystal structures of clinokurchatovite (a,b) and kurchatovite (c,d) and consisting of diborate groups (divided along the dashed lines as shown in Figures 1 and 2). The dot-and-dash lines in (a,c) indicate the relative positions of the B' and B'' of different orientations (distinguished by the “+” and “–” signs).

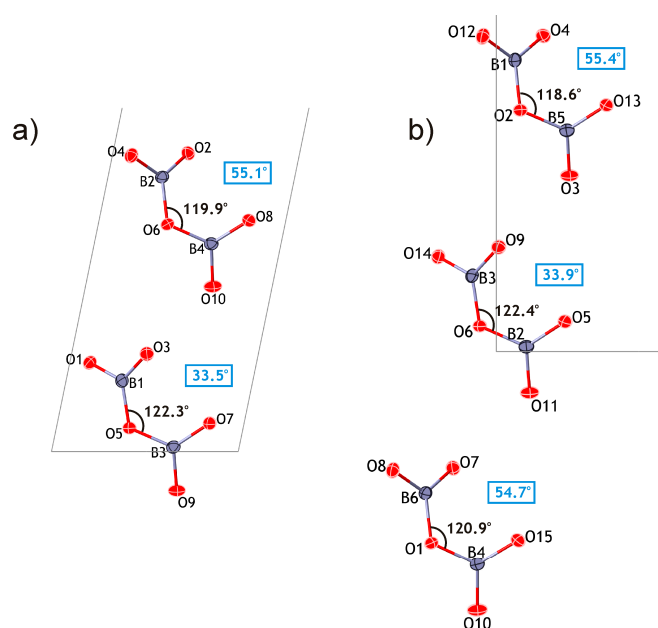


Figure 5. The arrangements of diborate groups in the crystal structures of kurchatovite (a) and clinokurchatovite (b), featuring their angular characteristics (the B–O–B angles are shown in black; the values in blue boxes correspond to the δ angles between the planes of the adjacent BO_3 triangles).

4. Discussion

According to Guinier et al. [21], “... an element or compound is polytypic if it occurs in several different structural modifications, each of which may be regarded as built up by stacking layers of (nearly) identical structure and composition, and if the modifications differ only in their stacking sequence”. This definition implies that the two structures belong to the same polytypic family if they: (1) contain nearly identical layers; (2) differ only in the stacking sequence. While the crystal structures of kurchatovite and clinokurchatovite conform to the first requirement, that is, they are built up from layers of the same kind, they do not conform to the second requirement, since the two structures cannot be obtained from one another simply by changing the stacking sequence. It is possible to obtain the crystal structure of kurchatovite from that of clinokurchatovite by the following sequence of operations: (a) splitting the structure of the latter into modules consisting of three 6 Å-blocks having the $\mathbf{B}':\mathbf{B}''$ ratio of 2:1; (b) stacking the modules in such a way that the adjacent modules are in different orientations, which can also be described as a chemical twinning [22,23]. According to the modular approach [22], this procedure for obtaining kurchatovite from clinokurchatovite means that the crystal structure of clinokurchatovite may be considered a basic structure, whereas that of kurchatovite is a derivative structure. Thus, the two minerals are not polytypes of one another; instead their relationship is better understood in terms of modular polymorphism. Re-definition of the two mineral species is not warranted. It is noteworthy that the situation would be very different if the crystal structures of kurchatovite and clinokurchatovite were to have the same $\mathbf{B}':\mathbf{B}''$ ratio. The veatchite polytypes [24] are an example of polytypism in which two types of layers are involved in borate minerals, but overall such polytypism is very rare.

The description in terms of the $\mathbf{B}':\mathbf{B}''$ blocks raises the important question about the potential occurrence of other members of the family consisting of the same elements. Considering the sequences of blocks in the two structures, two empirical rules can be derived:

(i) the \mathbf{B}'' blocks are always surrounded by the \mathbf{B}' blocks of the same directionality (i.e., of the same sign);

(ii) the B' blocks may occur in two combinations: either surrounded by two B'' blocks of the same sign or by one B'' block of the same sign and one B' block of the different sign. Thus, the following eight triplets are allowed that satisfy the (i) and (ii) conditions:

$$\begin{array}{llll} \text{I } (+B')(+B'')(+B') & \text{II } (-B')(-B'')(-B') & \text{III } (+B'')(+B')(+B'') & \text{IV } (-B'')(-B')(-B'') \\ \text{V } (+B'')(+B')(-B') & \text{VI } (-B')(+B')(+B'') & \text{VII } (-B'')(-B')(+B') & \text{VIII } (+B')(-B')(-B'') \end{array}$$

The number of symbolic sequences that may contain these triplets is obviously infinite, and the sequences may be both periodic and aperiodic. We note that, to produce a sequence that satisfy the rules, two triplets should overlap in two symbols: two right symbols of the first (preceding) one and two left symbols of the second (following) one. Thus, all the triplets can be split into the following ten overlapping pairs (see an example in Figure 6a):

$$\text{I-III II-IV I-V II-VII III-I IV-II V-VIII VI-I VII-VI VIII-II}$$

The relations between the triplets are illustrated in Figure 6b, which represents an analogue of de Bruijn diagram for cellular automata [25–27] that was considered as a model of crystallization processes [28,29]. The arrow lines in the diagram indicate the only possible sequence of triplets starting at the preceding triplet and ending at the following. Any realizable symbolic sequence is produced by the loop of arrows starting and ending at the same triplet.

Let us consider the possible symbolic sequences and their structural realizations in more detail:

1. The overlapping periodic sequences $\text{I} \leftrightarrow \text{III}$, $\text{III} \leftrightarrow \text{I}$, $\text{II} \leftrightarrow \text{IV}$ and $\text{IV} \leftrightarrow \text{II}$ (Figure 6c) produce the structure of clinokurchatovite. This is the simplest structure possible in this group and contains two blocks within its identity period (e.g., $[(+B')(+B'')]$).

2. Starting from triplet I and going to triplet V and so forth results in the following 6-membered sequence $\dots \rightarrow \text{VI} \rightarrow [\text{I} \rightarrow \text{V} \rightarrow \text{VIII} \rightarrow \text{II} \rightarrow \text{VII} \rightarrow \text{VI}] \rightarrow \text{I} \rightarrow \dots$ (Figure 6d), which corresponds exactly to the 6-membered sequence of blocks observed in the crystal structure of kurchatovite.

3. An infinite number of periodic and aperiodic sequences can be obtained by inserting into the 6-membered sequence of triplets given above any even subsequence from the sequences $\text{I} \leftrightarrow \text{III}$ and $\text{II} \leftrightarrow \text{IV}$. For instance, the sequence $[\text{I} \rightarrow \text{V} \rightarrow \text{VIII} \rightarrow \text{II} \rightarrow (\text{IV} \rightarrow \text{II}) \rightarrow \text{VII} \rightarrow \text{VI}]$ is produced by the inserting of the $(\text{IV} \rightarrow \text{II})$ element into the sequence $[\text{I} \rightarrow \text{V} \rightarrow \text{VIII} \rightarrow \text{II} \rightarrow \text{VII} \rightarrow \text{VI}]$ after the triplet II. However, all such derivative sequences are at least two blocks longer than the sequence producing kurchatovite.

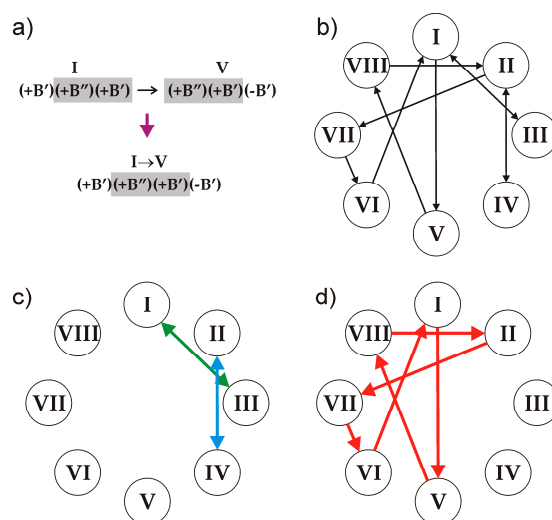


Figure 6. The illustration of the rule of overlapping triplets using the example of the I–V pair (a), the diagram of relations between the triplets (b), and the parts of diagram that result in the generation of clinokurchatovite (c) and kurchatovite (d) structures. See text for details.

Therefore, the following important conclusion is in order: given the rules (i) and (ii), the sequences of blocks observed in the crystal structures of clinokurchatovite and kurchatovite contain the minimal number of blocks per identity period. All other sequences are either aperiodic or contain at least two more blocks within their identity periods. It is remarkable that the natural structures are observed for the minimal possible periodic sequences only.

The information-theoretic analysis of structural complexity of the two minerals [23,30] shows that clinokurchatovite ($I_G = 4.170$ bits/atom and $I_{G,total} = 300.235$ bits/cell) is structurally simpler than kurchatovite ($I_G = 4.755$ bits/atom and $I_{G,total} = 1027.056$ bits/cell). A greater complexity for the derivative structure is to be expected given the proposed modular relationship between the two structures and the fact that the sequence of blocks in kurchatovite is 6-membered, whereas that in clinokurchatovite is 2-membered. According to the complexity-based classification of minerals proposed by Krivovichev [30], clinokurchatovite is intermediate, whereas kurchatovite is very complex. As it has been shown above, all other periodic structures in the “kurchatovite family” would contain at least 8-membered sequences of blocks and therefore would be even more structurally complex than kurchatovite.

Grew et al. [31] examined structural complexity of boron minerals in detail and reported the average Shannon information content per unit cell for this class of minerals as 340 bits/cell (i.e., close to the value found for clinokurchatovite). In fact, 46% of all boron minerals are intermediate in complexity (100 to 500 bits/cell), whereas only 3% are very complex (>1000 bits/cell). The reasons for the high structural complexity of kurchatovite can be inferred from the modular character of its structure, which is one of the most common mechanisms for the formation of complex crystal structures [30,31].

5. Conclusions

In conclusion, our study shows that kurchatovite and clinokurchatovite are not polytypes, but polymorphs and therefore re-consideration of their status as of separate mineral species is not warranted. However, the structures of the two minerals are closely related: the crystal structure of kurchatovite may be considered as a derivative of clinokurchatovite through the modular approach. In fact, we have demonstrated that, considering common structural features of kurchatovite and clinokurchatovite, the whole family of periodic and aperiodic structures can be generated. However, the two minerals under consideration possess the simplest periodic structures possible for the family, whereas all other structures would be structurally more complex. This may explain the absence of other “kurchatovite”-like polymorphs of CaMgB_2O_5 in nature: only simplest structures from the infinite array of possible configurations are realized. This might be viewed as a consequence of the maximum-entropy principle (since information-based structural complexity provides a negative contribution to configurational entropy [32]) or as a result of the least-action principle, which was expressed by Pierre Louis Maupertouis as “nature is thrifty in all its actions”

This study also demonstrates that diversity and complexity of mineral structures involve different and sometimes complicated structural combinatorics, from which combinatorics of polytypes is just a single and relatively simple branch.

Supplementary Materials: The following are available online at <http://www.mdpi.com/2075-163X/8/8/332/s1>, Crystallographic Information Files (CIFs) for kurchatovite and clinokurchatovite.

Author Contributions: Conceptualization, S.V.K. and E.S.G.; Methodology, S.V.K. and I.V.P.; Investigation, Y.A.P., S.V.K., I.V.P. and V.O.Y.; Writing—Original Draft Preparation, Y.A.P., S.V.K., I.V.P., and E.S.G.; Writing—Review and Editing, S.V.K. and E.S.G.; Visualization, S.V.K.

Funding: This research was funded by the Russian Foundation for Basic Research (in part of X-ray studies; grant 17-05-01027 to Y.A.P. and S.V.K.) and Presidium of the Russian Academy of Sciences (in part of complexity analysis).

Acknowledgments: The X-ray diffraction studies were performed in the X-ray Diffraction Resource Centre of St. Petersburg State University.

Conflicts of Interest: The authors declare no conflict of interest.

References

1. Malinko, S.V.; Khalturina, I.I.; Ozol, A.A.; Bocharov, V.M. *Boron Minerals. Handbook*; Nedra: Moscow, Russia, 1991. (In Russian)
2. Aleksandrov, S.M. Genesis and composition of ore-forming magnesian borates, their analogues, and modifications. *Geochem. Int.* **2003**, *41*, 440–458.
3. Grew, E.S.; Hystad, G.; Hazen, R.M.; Golden, J.; Krivovichev, S.V.; Gorelova, L.A. How many boron minerals occur in Earth's upper crust? *Am. Mineral.* **2017**, *102*, 1573–1587. [[CrossRef](#)]
4. Hayashi, A.; Momma, K.; Miyawaki, R.; Tanabe, M.; Kishi, S.; Kobayashi, S.; Kusachi, I. Kurchatovite from the Fuka mine, Okayama Prefecture, Japan. *J. Mineral. Petrol. Sci.* **2017**, *112*, 159–165. [[CrossRef](#)]
5. Malinko, S.V.; Lisytsyn, A.E.; Dorofeeva, K.A.; Ostrovskaya, I.V.; Shashkin, D.P. Kurchatovite, a new mineral. *Zap. Vses. Min. Obshch.* **1966**, *95*, 203–209. (In Russian)
6. Pekov, I.V. *Minerals First Discovered on the Territory of the Former Soviet Union*; Ocean Pictures: Moscow, Russia, 1998; ISBN 978-5900395166.
7. Yakubovich, O.V.; Simonov, M.A.; Belokoneva, E.L.; Egorov-Tismenko, Y.K.; Belov, N.V. Crystalline structure of Ca, Mg-diorthotriborate (pyroborate) kurchatovite $\text{CaMg}[\text{B}_2\text{O}_5]$. *Dokl. Akad. Nauk. SSSR* **1976**, *230*, 837–840. (In Russian)
8. Nikolaychuk, G.V.; Nekrasov, I.Y.; Shashkin, D.P. Hydrothermal synthesis of kurchatovite in the system $\text{CaO-MgO-B}_2\text{O}_3\text{-H}_2\text{O}$. *Dokl. Akad. Nauk. SSSR* **1970**, *190*, 139–141. (In Russian)
9. Borodanov, V.M.; Malinko, S.V. Twins of kurchatovite. *Zap. Vses. Min. Obshch.* **1971**, *100*, 356–357. (In Russian)
10. Malinko, S.V.; Shashkin, D.P.; Yurkina, K.V.; Bychov, V.P. New data on kurchatovite. *Zap. Vses. Min. Obshch.* **1973**, *102*, 696–702. (In Russian)
11. Malinko, S.V.; Pertsev, N.N. Rhombohedral, monoclinic kurchatovite; new data. *Zap. Vses. Min. Obshch.* **1979**, *108*, 595–599. (In Russian)
12. Yakubovich, O.V.; Yamnova, N.A.; Shchedrin, B.M.; Simonov, M.A.; Belov, N.V. The crystal structure of magnesium kurchatovite, $\text{CaMg}[\text{B}_2\text{O}_5]$. *Dokl. Akad. Nauk. SSSR* **1976**, *228*, 842–845. (In Russian)
13. Yakubovich, O.V.; Simonov, M.A.; Belov, N.V. Crystal-structure of synthetic Mn-kurchatovite, $\text{CaMn}[\text{B}_2\text{O}_5]$. *Dokl. Akad. Nauk. SSSR* **1978**, *238*, 98–100. (In Russian)
14. Gorshenin, A.D.; Pertsev, N.N.; Organova, N.I.; Laputina, I.P.; Nikitina, I.B. Find of monoclinic kurchatovite and cubic harkerite with low silicon content in the Balkhash region. *Dokl. Earth Sci.* **1977**, *236*, 170–173.
15. Simonov, M.A.; Egorov-Tismenko, Y.K.; Yamnova, N.A.; Belokoneva, E.L.; Belov, N.V. Crystal structure of natural monoclinic kurchatovite $\text{Ca}_2(\text{Mg}_{0.86}\text{Fe}_{0.14})(\text{Mg}_{0.92}\text{Fe}_{0.08})[\text{B}_2\text{O}_5]_2$. *Dokl. Akad. Nauk SSSR* **1980**, *251*, 1125–1128. (In Russian)
16. Malinko, S.V.; Pertsev, N.N. Clinokurchatovite; new structural modification of kurchatovite. *Zap. Vses. Min. Obshch.* **1983**, *112*, 483–487. (In Russian)
17. Callegari, A.; Mazzi, F.; Tadini, C. Modular aspects of the crystal structures of kurchatovite and clinokurchatovite. *Eur. J. Mineral.* **2003**, *15*, 277–282. [[CrossRef](#)]
18. Belokoneva, E.L. OD family of Ca,Mg-borates of the kurchatovite group. *Crystallogr. Rep.* **2003**, *48*, 222–225. [[CrossRef](#)]
19. Sheldrick, G.M. Crystal structure refinement with *SHELXL*. *Acta Crystallogr.* **2015**, *C71*, 3–8.
20. Filatov, S.K.; Bubnova, R.S. Borate crystal chemistry. *Phys. Chem. Glas.* **2000**, *41*, 216–224.
21. Guinier, A.; Bokij, G.B.; Boll-Dornberger, K.; Cowley, J.M.; Durovič, S.; Jagodzinski, H.; Krishna, P.; de Wolff, P.M.; Zvyagin, B.B.; Cox, D.E.; et al. Nomenclature of polytype structures. Report of the International Union of Crystallography Ad-Hoc Committee on the Nomenclature of Disordered, Modulated and Polytype Structures. *Acta Crystallogr.* **1984**, *A40*, 399–404. [[CrossRef](#)]
22. Ferraris, G.; Makovicky, E.; Merlino, S. *Crystallography of Modular Materials*; Oxford University Press: Oxford, UK, 2004; ISBN 9780198526643.
23. Krivovichev, S.V. Structure description, interpretation and classification in mineralogical crystallography. *Crystallogr. Rev.* **2017**, *23*, 2–71. [[CrossRef](#)]
24. Grice, J.D.; Pring, A. Veatchite: Structural relationships of the three polytypes. *Am. Mineral.* **2012**, *97*, 489–495. [[CrossRef](#)]
25. Sutner, K. De Bruijn graph and linear cellular automata. *Complex Syst.* **1991**, *5*, 19–30.

26. Krivovichev, S.V. Algorithmic crystal chemistry: A cellular automata approach. *Crystallogr. Rep.* **2012**, *57*, 10–17. [[CrossRef](#)]
27. Shevchenko, V.Y.; Krivovichev, S.V.; Tananaev, I.G.; Myasoedov, B.F. Cellular automata as models of inorganic structures self-assembly (Illustrated by uranyl selenate). *Glass Phys. Chem.* **2013**, *39*, 1–10. [[CrossRef](#)]
28. Krivovichev, S.V. Crystal structures and cellular automata. *Acta Crystallogr. A* **2004**, *60*, 257–262. [[CrossRef](#)] [[PubMed](#)]
29. Krivovichev, S.V. Actinyl compounds with hexavalent elements (S, Cr, Se, Mo)—Structural diversity, nanoscale chemistry, and cellular automata modeling. *Eur. J. Inorg. Chem.* **2010**, *2010*, 2594–2603. [[CrossRef](#)]
30. Krivovichev, S.V. Structural complexity of minerals: Information storage and processing in the mineral world. *Mineral. Mag.* **2013**, *77*, 275–326. [[CrossRef](#)]
31. Grew, E.S.; Krivovichev, S.V.; Hazen, R.M.; Hystad, G. Evolution of structural complexity in boron minerals. *Can. Mineral.* **2016**, *54*, 125–143. [[CrossRef](#)]
32. Krivovichev, S.V. Structural complexity and configurational entropy of crystals. *Acta Crystallogr. B* **2016**, *72*, 274–276. [[CrossRef](#)] [[PubMed](#)]



© 2018 by the authors. Licensee MDPI, Basel, Switzerland. This article is an open access article distributed under the terms and conditions of the Creative Commons Attribution (CC BY) license (<http://creativecommons.org/licenses/by/4.0/>).